Role of Cu^0 in Controlled/"Living" Radical Polymerization

Krzysztof Matyjaszewski,* Nicolay V. Tsarevsky, Wade A. Braunecker, Hongchen Dong, Jinyu Huang, Wojciech Jakubowski, Yungwan Kwak, Renaud Nicolay, Wei Tang, and Jeong Ae Yoon

Department of Chemistry, Carnegie Mellon University, 4400 Fifth Avenue, Pittsburgh, Pennsylvania 15213

Received August 7, 2007; Revised Manuscript Received August 17, 2007

ABSTRACT: Several propositions have been made about the mechanism in which Cu^0 mediates controlled radical polymerization that include (1) exclusive activation of an alkyl halide initiator by exceptionally active Cu^0 to generate a propagating radical and a Cu^I species, (2) instantaneous disproportionation of Cu^I into Cu^0 and Cu^{II} in "catalytic" solvents such as DMSO, and (3) deactivation of the radical by Cu^{II} to establish an equilibrium between active and dormant polymer chains. It was further postulated that the activation and deactivation processes in this technique, entitled single-electron-transfer living radical polymerization (SET-LRP), occur via outer-sphere electron transfer (OSET) to produce alkyl halide radical anion intermediates. We report herein on our own investigation of the aforementioned mechanism using Cu complexes of tris[2-(dimethylamino)ethyl]amine (Me_6TREN). Model studies were employed to quantify disproportionation of Cu^I/Me_6TREN in DMSO, DMF, and MeCN, where comproportionation of Cu^0 with Cu^{II} to form Cu^I was slow but dominant in all three solvents. Relative activation rates of alkyl halides by Cu^0 and Cu^I with Me_6TREN were studied; reactions catalyzed by Cu^I/Me_6TREN were significantly faster than those employing Cu^0. Polymerization of methyl acrylate proceeded in a similar manner in both DMSO and MeCN at 25 °C initiated by an alkyl halide using either Cu^0 and Me_6-TREN, Cu^I/Me_6TREN, or a slow dosing of Cu^I/Me_6TREN. These studies ultimately indicate that in addition to slowly activating alkyl halides Cu^0 also acts as a reducing agent, regenerating Cu^I activator from accumulated Cu^{II}, thereby emulating the mechanism activators regenerated by electron transfer in atom transfer radical polymerization (ARGET ATRP). The possibility of OSET among copper species and alkyl halides was evaluated on the basis of literature data and found to be negligible in comparison to an atom transfer process (i.e., inner-sphere electron transfer).

Introduction

The extensive development of controlled radical polymerization techniques in the past decade has ultimately provided synthetic polymer chemists with the necessary means to craft a host of unique materials otherwise unattainable with conventional polymerization methods.[1−4] One technique in particular, atom transfer radical polymerization (ATRP),[5] has been exceptionally useful in the preparation of various (co)polymers of precise composition, topology, and functionality,[6−13] of both high and low molecular weight, and from a large variety of monomers, including styrenes, acrylates, methacrylates, acrylamides, acrylonitrile, vinyl acetate, and others.[5,14−20] Several recent advances have been made (discussed herein) that allow the overall required concentration of ATRP metal catalyst to be lowered from parts per thousand to parts per million.[21−23] These new developments have generated much enthusiasm for those interested in adopting ATRP on an industrial scale.[24] Of course, any optimization of the methods will necessitate a thorough understanding of their mechanism.

The "living" nature of polymer chains in ATRP arises from an equilibrium between propagating radicals $R^\bullet$ and dormant halide capped chains R−X that is established with the aid of a transition metal catalyst.[5] Homolytic cleavage of R−X by a metal complex activator Mt^n/L generates (with an activation rate constant k_{act}) the corresponding higher oxidation state metal halide complex deactivator $X-Mt^{n+1}$/L and a radical $R^\bullet$. (A representative example of this process is illustrated in Scheme 1, where the values of the rate constants refer to a styrene polymerization at 110 °C catalyzed by Cu^IBr/2,2-bipyridine.[25−27]) $R^\bullet$ can then propagate with a vinyl monomer (k_p), terminate with another $R^\bullet$ (k_t), or be reversibly deactivated in this equilibrium by $X-Mt^{n+1}$/L (k_{deact}). While termination reactions are ultimately curbed by the persistent radical effect,[27−29] they are always present to some degree in any radical polymerization process. Under normal ATRP conditions, between 1 and 10% of chains terminate, which is precisely why a high catalyst concentration is required to reach high conversions. Every act of radical−radical termination irreversibly consumes 2 equiv of the Cu^I activator, and without a sufficient starting catalyst concentration, polymerization would cease at low conversion once all of the activator was consumed.

The rate of polymerization in ATRP is governed by a ratio of the concentration of activator to deactivator (i.e., $[Mt^n/L]/[XMt^{n+1}/L]$) according to eq 1.[25]

$$R_p = k_p[M][R^\bullet] = k_p[M]K_{ATRP}[R-X]([Mt^n/L]/[XMt^{n+1}/L]) \quad (1)$$

In principle, therefore, the absolute amount of metal catalyst can be decreased without affecting the rate of polymerization. However, fast rates cannot be maintained without a sufficient absolute amount of catalyst under normal ATRP conditions due to the aforementioned radical termination reactions. By effectively employing Cu^0 or Fe^0 as reducing agents to lower the amount of accumulated Cu^{II} by reducing it to Cu^I, it was demonstrated that ATRP could be made significantly faster.[30−34] This concept was essentially the precursor to a new technique known as activators regenerated by electron transfer (ARGET)

* Corresponding author. E-mail: km3b@andrew.cmu.edu.

10.1021/ma0717800 CCC: $37.00
Published on Web 10/05/2007

Scheme 1. Representitive ATRP Equilibrium

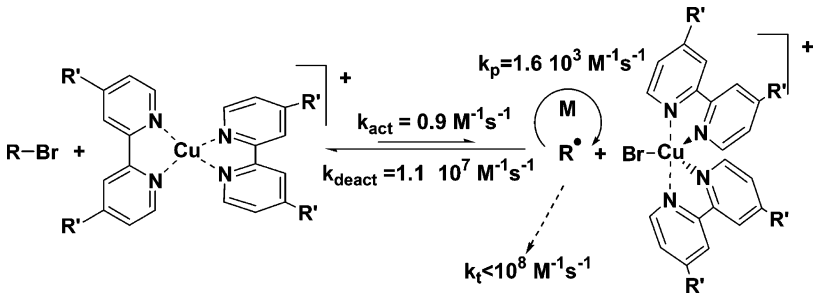

Scheme 2. Postulated SET-LRP and ARGET ATRP Mechanisms

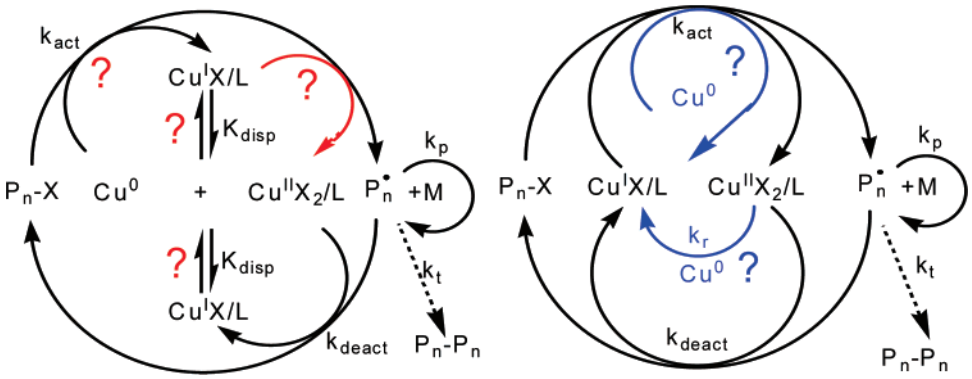

ATRP,[21,35–39] for which it was demonstrated that the overall concentration of metal catalyst could be dramatically lowered (to 1−50 ppm) while maintaining control over the polymerization to high conversion by employing organic reducing agents such as sugars, ascorbic acid, hydrazine, amines, and phenols to maintain an appropriate balance of [Cu^I] and [Cu^{II}]. Free radical initiators such as AIBN were employed in a similar way to reduce Cu^{II} with a slow dosing of radicals in a method known as initiators for continuous activator regeneration (ICAR) ATRP.[22]

Recently, a system using Cu^0 in the presence of tris[2-(dimethylamino)ethyl]amine (Me_6TREN) ligand was applied to the polymerization of vinyl chloride (VC).[40,41] High molecular weight polymers of methyl acrylate (MA) were also prepared with this technique in a relatively short time (a few hours or less) using DMSO as the solvent and an amount of Cu^0 ranging from parts per thousand to parts per million.[42] A new mechanism was proposed to occur under these conditions, entitled single-electron-transfer living radical polymerization (SET-LRP), that was postulated to involve (1) exclusive activation of R−X by an exceptionally active Cu^0 species to generate (in the presence of complexing ligand) R• and a Cu^IX species, (2) instantaneous disproportionation of two Cu^IX into Cu^0 and $Cu^{II}X_2$ in "catalytic" solvents such as DMSO, and (3) deactivation of R• by $Cu^{II}X_2$ to establish an equilibrium between active and dormant polymer chains. (Note that the Cu^I- and Cu^{II}-containing species are complexed with a ligand L which is omitted for simplicity.) The proponents of SET-LRP contend the activation and deactivation processes in this technique occur via outer-sphere electron transfer (OSET) to produce alkyl halide radical anion intermediates and the corresponding Cu^I cations and furthermore that SET-LRP is somehow less susceptible to side reactions and radical termination as some function of the process occurring via OSET (in contrast to normal ATRP, which they accept as occurring via inner-sphere electron transfer (ISET), where the activation of R−X by Cu^I and subsequent generation of Cu^{II} is accompanied via a halogen-bridged transition state). The SET-LRP mechanism as presented in ref 42 is illustrated in Scheme 2, supplemented with a half-circle arrow representing direct activation by Cu^I and with question marks related to the extent of disproportionation of Cu^I and activation by Cu^0. The ARGET ATRP mechanism[21,35] is represented in parallel fashion, where Cu^0 principally serves to regenerate Cu^I and where activation occurs predominantly by Cu^I. (Of course, a small contribution of the direct reaction between alkyl halides and Cu^0 must initially take place.)

From strictly a thermodynamic perspective, the dominant role of Cu^0 in either of these proposed mechanisms is not immediately clear. Consider an energy level diagram (Figure 1) containing all relevant intermediate species in the SET-LRP and ARGET ATRP mechanisms, where the same number of each type of atom is included in each step so that valid relative comparisons of the energies can be made. It is well-known that deactivation of R• by $Cu^{II}X_2$ complexes with a ligand to give Cu^IX and R−X (as in reverse ATRP[43]) favors the dormant side of the ATRP equilibrium (Cu^IX + R−X, see Scheme 1),[9] or else the polymerization would not be "living". Thus, the products of this reaction are significantly lower in energy than the starting materials, as illustrated in Figure 1 (an extra Cu^IX is included in the products and reactants in order to keep the number of halogen and copper atoms constant for each step in this figure). Spontaneous disproportionation of two Cu^IX molecules into Cu^0 and $Cu^{II}X_2$, as required by the SET-LRP mechanism, suggests the energy of the products of disproportionation must be lower still, as presented on the right-hand side of Figure 1. Since no significant deactivation of a R• by Cu^IX is reported to occur in the literature, the activation barrier for this process must be larger than that for deactivation of a R• by $Cu^{II}X_2$. Looking at the activation barriers of the steps in reverse, it should be easier for Cu^IX rather than Cu^0 to activate R−X. Thus, if disproportionation is not complete (governed by the equilibrium constant for disproportionation), Cu^IX should dominate in the role as activator.

Cu^0 in the presence of a ligand is certainly capable of activating alkyl halides.[30,44,45] Therefore, the left-hand side of Figure 1 suggests that in solvents such as acetonitrile, where there is virtually no disproportionation of Cu^IX, Cu^0 would be the more active species from a thermodynamic point of view.

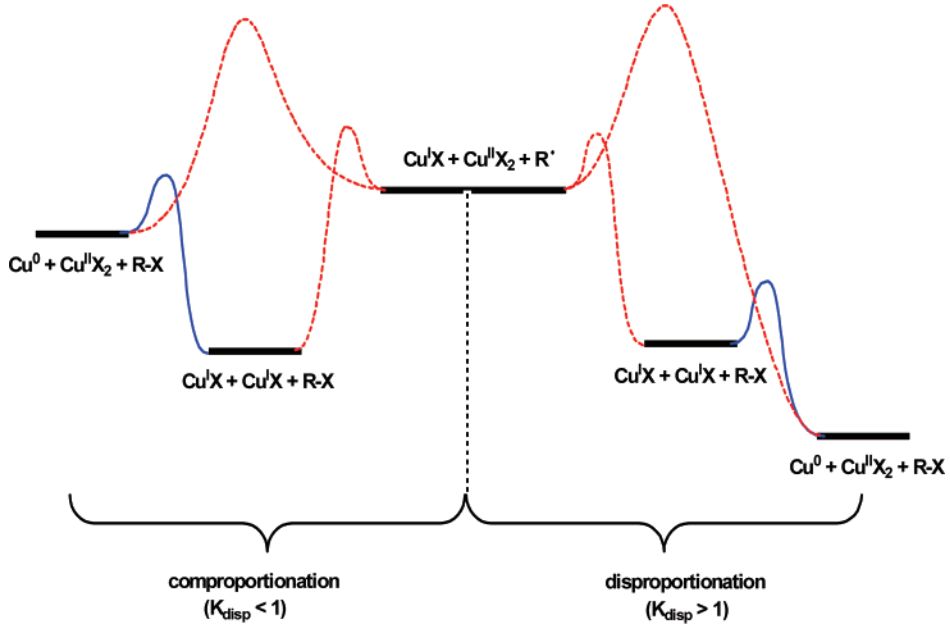

Figure 1. Illustration of hypothetical activation barriers and energy levels for the activation of RX by Cu^0 or Cu^IX when disproportionation or comproportionation dominates (the complexing ligand L is omitted in this figure for clarity).

Scheme 3. Activation/Deactivation and Disproportionation/Comproportionation Equilibria in the $Cu^0-Cu^IX-Cu^{II}X_2-RX$ System

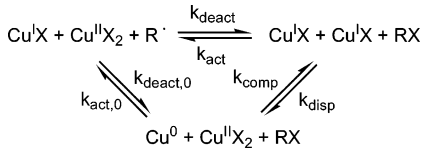

However, Cu^0 can also act as a reducing agent to comproportionate with $Cu^{II}X_2$ and return Cu^IX activator to solution (as proposed in ARGET ATRP). Whether the overall preferred (lower energy) pathway for activation of R−X will proceed through comproportionation and subsequent activation by Cu^I vs a direct reaction with Cu^0 will depend in part upon the relative activation barriers for reduction of $Cu^{II}X_2$ compared with activation of R−X. Additionally, whether Cu^0 is responsible for activating more or less polymer chains than Cu^IX will also depend upon the surface area of the insoluble Cu^0 catalyst.

The three equilibria from Figure 1, which coexist in the reaction system, can be conveniently presented as the cycle shown in Scheme 3.

The principle of microscopic reversibility (PMR)[46−48] demands that five of the six rate constants for the processes shown in Scheme 3 be independent, while the sixth one is related to the other five via eq 2.

$$k_{act,0}k_{deact}k_{disp} = k_{deact,0}k_{comp}k_{act} \tag{2}$$

The application of the PMR to the system in Scheme 3 leads to some important conclusions. First, the equilibrium constant of the process of activation of alkyl halide RX by Cu^0 and deactivation of the produced radical by Cu^IX, which can be termed K^0_{ATRP}, depends upon the "standard" ATRP equilibrium constant (RX activation by Cu^IX and radical deactivation by $Cu^{II}X_2$) and the extent to which Cu^IX disproportionates. These constants will be very much solvent- and ligand-dependent:

$$\frac{k_{act,0}}{k_{deact,0}} \equiv K^0_{ATRP} = \frac{k_{comp}}{k_{disp}}\frac{k_{act}}{k_{deact}} = \frac{K_{ATRP}}{K_{disp}} \tag{3}$$

Equations 2 and 3 can further be rearranged in the form

$$\frac{k_{act,0}}{k_{act}} = \frac{k_{deact,0}}{k_{deact}}\frac{1}{K_{disp}} \tag{4}$$

It is known that $Cu^{II}X_2$ is a better deactivator than Cu^IX species ($k_{deact} \gg k_{deact,0}$).[49−51] Consequently, the PMR dictates according to eq 4 that activation must be significantly faster with Cu^IX than with Cu^0 ($k_{act} \gg k_{act,0}$) for systems that favor disproportionation ($K_{disp} > 1$). Thus, the proposed SET-LRP mechanism,[42] with preferred deactivation by $Cu^{II}X_2$ ($k_{deact} > k_{deact,0}$), preferred activation by Cu^0 ($k_{act,0} > k_{act}$), and dominating disproportionation ($K_{disp} > 1$), violates the PMR.

We were therefore prompted to reinvestigate the predominant role of Cu^0 in living radical polymerization in several organic solvents. The equilibrium constant of disproportionation K_{disp}, which is related to the relative energies of $Cu^IX + Cu^IX$ and $Cu^0 + Cu^{II}X_2$ in Figure 1, is reported hereafter for various solvents and measured in the presence of ligand (where K_{disp} becomes K^L_{disp}, see eq 6). K_{disp} can also be calculated from the Nernst equation knowing the redox potentials of the Cu^I/Cu^0 and Cu^{II}/Cu^I couples (see eq 5, where R is the universal gas constant (1.987 cal mol^{-1} K^{-1}), T is the absolute temperature, and F is the Faraday constant (96 500 C mol^{-1})).

$$\log K_{disp} = \frac{E^0(Cu^I/Cu^0) - E^0(Cu^{II}/Cu^I)}{2.303RTF^{-1}} \tag{5}$$

We also compare the kinetics of the activation processes by Cu^0 and Cu^IX with additional model studies, test the polymerization of MA in DMSO and MeCN (solvents in which disproportionation of Cu^I and comproportionation of Cu^0 and Cu^{II} are dominant, respectively, according to ref 42), and evaluate the effectiveness of various Cu^0 species as polymerization catalysts. We also evaluate, on the basis of available literature data, the possibility of outer-sphere electron transfer between copper species and alkyl halides.

Experimental Section

Materials. Tris[2-(dimethylamino)ethyl]amine (Me_6TREN) was synthesized according to literature procedures.[52] All other Cu

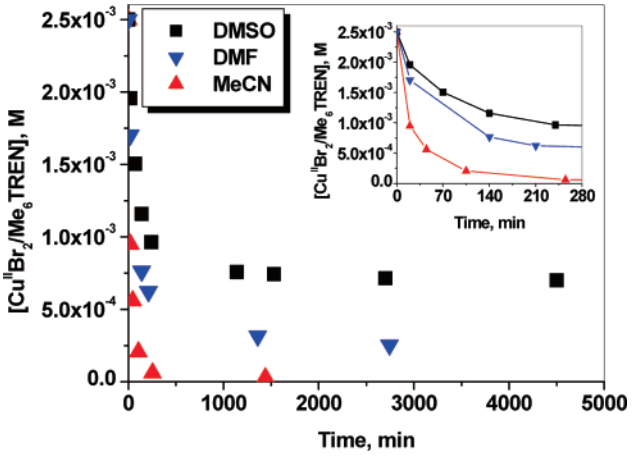

Figure 2. Comproportionation of $Cu^{II}Br_2/Me_6TREN$ (initial concentration 2.5 mM) in the presence of Cu^0 (10% excess) and Me_6TREN (concentration equal to the total amount of Cu) at 25 °C in MeCN, DMSO, and DMF. The inset is an expansion of the first 4 h.

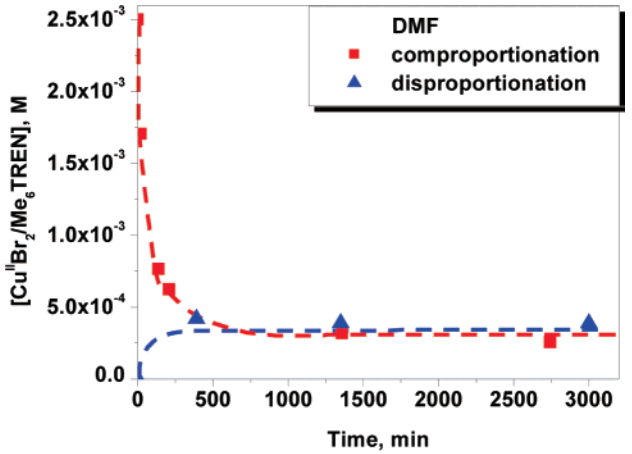

Figure 3. Comproportionation of $Cu^{II}Br_2/Me_6TREN$ (initial concentration 2.5 mM) in the presence of Cu^0 (10% excess) and disproportionation of 5.0 mM $Cu^{I}Br/Me_6TREN$ in DMF at 25 °C. The dashed lines do not represent a fit of the data but rather are present to guide the eye.

complexes, reagents, and solvents used in this study were obtained from Aldrich. Methyl acrylate (MA) was passed through a column filled with basic alumina to remove inhibitor. All monomers, ligands, and solvents were deoxygenated by purging with nitrogen for at least 1 h prior to usage. Cu^0 powder (<75 μm in diameter) was used in all model studies and polymerizations, unless otherwise specified.

Analyses. Monomer conversions were determined using a Shimadzu GC 14-A gas chromatograph equipped with a FID detector and J&W Scientific 30 m DB WAX Megabore column. Molecular weights and molecular weight distributions were determined on a gel permeation chromatography (GPC) system consisting of a Waters 515 pump, a Waters 717plus autoinjector, Polymer Standards Service columns (Styrogel 10^5, 10^3, 10^2 Å), and a Waters 2410 RI detector against polystyrene standards using THF as the eluent at a flow rate of 1 mL/min (35 °C). All spectroscopic measurements were performed on a Cary 5000 UV/vis/NIR spectrometer (Varian).

Comproportionation Experiments. $Cu^{II}Br_2$ (0.0056 g, 0.025 mmol) and Cu^0 powder (<75 μm, 0.0017 g, 0.0275 mmol) were weighed on a small glass slide, which was inserted and left in a Schlenk flask. The flask was closed with a stopper attached to a quartz cuvette and was then evacuated and backfilled with nitrogen several times. Deoxygenated solvent (10 mL) was added (concentration of Cu^{II} was 2.5 mM) followed by Me_6TREN (13.9 μL, 0.0525 mmol; 1 equiv vs the total Cu). In other experiments, different amounts of ligand were used. The reaction mixture was stirred in a water bath at 25 °C, and spectra were collected at various time intervals. Before collecting the spectrum, the flask with the cuvette was placed inside the spectrometer and left there for 10 min to allow precipitation of any insoluble material. The decrease in the $Cu^{II}Br_2/Me_6TREN$ concentration was monitored from the absorption at 970 nm. The extinction coefficients of the complex at this wavelength in the presence of 1−2 equiv excess of ligand were measured separately and were 439.5, 458.1, and 471.7 M^{-1} cm^{-1} in MeCN, DMF, and DMSO, respectively. Similar experiments were carried out using the $CuCl_2/Me_6TREN$ complex in DMSO; the absorbance maximum of this complex in DMSO in the presence of 1−2 equiv of ligand was at 940 nm, $\epsilon_{940} = 499.1$ M^{-1} cm^{-1}.

Representative Polymerization. A Schlenk flask was charged with Cu^0 or $Cu^{I}Br$ (0.0435 mmol). It was then closed, evacuated, and back-filled with nitrogen several times, and deoxygenated MA (9 mL, 96.6 mmol), Me_6TREN (11.5 μL, 0.0435 mmol), and DMSO or MeCN (4.5 mL) were added. After four freeze−pump−thaw cycles, the flask was filled with nitrogen. After melting the reaction mixture and warming to room temperature, an initial sample was taken and the sealed flask was placed in a thermostated oil bath at 25 °C. The initiator methyl 2-bromopropionate (MBP) (48.5 μL, 0.435 mmol) was then added into the solution to start the reaction. Samples were taken at timed intervals and analyzed by GC and GPC to follow the progress of the reaction.

Slow Dosing of $CuBr/Me_6TREN$. MA and DMSO or MeCN were deoxygenated by bubbling with nitrogen for 1 h. $Cu^{II}Br_2$ (0.279 mg, 1.25×10^{-6} mol), Me_6TREN (0.33 μL, 1.25×10^{-6} mol), DMSO or MeCN (1.9 mL), and anisole (0.5 mL as internal standard) were injected from a stock solution into a nitrogen-purged flask. MA (4.5 mL, 50 mmol) was added, and an initial sample was taken against which conversion would be monitored. After the flask was placed in a 25 °C thermostated oil bath, MBP (5.22 mg, 0.0313 mmol in 0.625 mL of DMSO) was added. A solution of $Cu^{I}Br$ (3.59 mg, 0.0250 mmol) and Me_6TREN (6.6 μL, 0.0250 mmol) in 2.1 mL of DMSO was then added over 5 h. Samples were taken at timed intervals and analyzed by GC and GPC to follow the progress of the reaction.

Model Studies of Activation. A 10.0 mM stock solution of $PhCH_2Cl$ (12.6 mg, 0.1 mmol) was prepared with 18.1 mg (0.1 mmol) of trichlorobenzene (TCB) internal standard in 10.0 mL of MeCN. 9.9 mg (0.1 mmol) of $Cu^{I}Cl$ was added to a separate Schlenk flask, and the flask was evacuated and back-filled with nitrogen several times. 3 mL of nitrogen purged MeCN was then added to the Schlenk flask. In a 10 mL round-bottom flask, 23.0 mg of Me_6TREN (0.1 mmol) along with 1 mL of MeCN was added, subjected to three freeze−pump−thaw cycles, and then transferred to the Schlenk flask with Cu via a nitrogen-purged syringe. Finally, 1 mL of the $PhCH_2Cl$ and TCB stock solution and 15.6 mg of TEMPO (0.1 mmol) were added to another 10 mL round-bottom flask and degassed by three freeze−pump−thaw cycles. After this solution was transferred to the Schlenk flask via a nitrogen-purged syringe, the reaction began. A time zero sample was immediately taken for GC analysis. The heterogeneous reaction was carried out at room temperature with constant stirring. Samples were taken at timed intervals to monitor (by GC) consumption of $PhCH_2Cl$ with time. GC was performed using a Schimadzu GC-17A, an AOC-20i autosampler, and a J&W Scientific DB 608 column (30 m × 0.53 mm) with a FID detector.

Model Equilibrium Studies. 3.8 mg (0.06 mmol) of Cu^0 was added to a Schlenk flask joined to a quartz UV cuvette. The Schlenk flask was carefully sealed. The flask was evacuated and backfilled with nitrogen five times. 3 mL of deoxygenated MeCN was added into the flask via a nitrogen-purged syringe through the sidearm. 11.5 mg (0.05 mmol) of Me_6TREN in 1 mL of MeCN was added to a round-bottom flask, subjected to three freeze−pump−thaw cycles, and then added to the Schlenk flask through the sidearm via a nitrogen-purged microsyringe. The contents were stirred until a colorless solution was obtained. In another round-bottom flask, 12.6 mg (0.05 mmol) of $PhCH_2Cl$ and 18.1 mg (0.05 mmol) of TCB along with 1 mL of MeCN were added and also subjected to

Table 1. Disproportionation Equilibrium Constants of Cu^IBr/Me_6TREN in Various Solvents at 25 °C

solvent	$[Cu^{II}Br_2]_0$, mM	$[Cu^0]_0$, mM	$[Me_6TREN]_0$, mM	$[Cu^{II}Br_2/Me_6TREN]_{eq}$, mM ($[Cu^{II}Br_2/Me_6TREN]_{eq}/[Cu^{II}Br_2]_0$)	log K^L_{disp}
DMSO	2.5	2.75	5.25	0.700 (0.280)	−1.29
DMSO	2.5	2.75	10.50	0.304 (0.122)	−1.04
DMSO	2.5	2.75	15.75	0.067 (0.027)	−1.51
DMF	2.5	2.75	5.25	0.254 (0.102)	−2.20
MeCN	2.5	2.75	5.25	<0.026 (<0.010)	<−4

three freeze−pump−thaw cycles. The initiator solution was then transferred to the Schlenk flask via a nitrogen-purged microsyringe. The absorbance at a wavelength corresponding to the λ_{max} of the generated $X-Cu^{II}$ complex was monitored at timed intervals. The concentration of the deactivator generated in the system was calculated using independently determined values of the extinction coefficients for the $Cu^{II}X_2/L_n$ complexes (X = halogen and L = ligand). Other combinations of alkyl halides and Cu^I complexes were studied in a similar fashion. At the same time, samples were taken at timed intervals to monitor the consumption of $PhCH_2Cl$ with time by GC.

Results and Discussion

I. Model Studies on Disproportionation. The solvent dependence of the disproportionation equilibrium for noncoordinated Cu ions has been thoroughly studied in the literature.[53] Values of K_{disp} as defined in eq 5 and obtained from electrochemistry range from 10^6 M^{-1} in water, where Cu^{II} is well solvated,[54,55] to 10^{-21} M^{-1} in acetontrile, where Cu^I is well stabilized.[56,57] In solvents such as DMSO, which have little "preference" to solvate either Cu^I or Cu^{II}, K_{disp} is near unity (0.2−0.3 M^{-1}).[58−60] In the presence of a complexing ligand L that stabilizes Cu^I and Cu^{II} to a different degree, the disproportionation process in eq 6 is influenced and characterized by a new equilibrium constant K^L_{disp} as shown in eq 7 for ligands forming 1:1 complexes (where K_{disp} is the equilibrium constant in the same solvent in the absence of L, and β^I and β^{II} are the stability constants of the Cu^I and Cu^{II} complexes with L, respectively).

$$2\,Cu^IL \overset{K^L_{disp}}{\rightleftharpoons} Cu^{II}L + Cu^0 + L \qquad (6)$$

$$K^L_{disp} = \frac{[Cu^{II}L][L]}{[Cu^IL]^2} = \frac{\beta^{II}}{(\beta^I)^2}K_{disp} \qquad (7)$$

Halide ions, which are always present in ATRP reactions, can coordinate to the Cu^{II} complex as well as form counterions of the coordinatively saturated Cu^I and $Cu^{II}X$ species. The effect of different counterions and their relative concentration on the disproportionation equilibrium is currently under investigation, and a few examples are illustrated in the Supporting Information, but a thorough study of this phenomenon is beyond the scope of this paper. The bromide ion is therefore used exclusively throughout this study, and in any calculation of disproportionation equilibrium constants, the bromide counterions are not treated as individual species.

Both comproportionation and disproportionation of Cu complexes were evaluated in model studies using Me_6TREN as a complexing ligand in several relevant solvents following rigorous deoxygenation. In disproportionation experiments, the Cu^I complex of Me_6TREN was formed in a deoxygenated solvent, and spectra were collected at timed intervals. The disproportionation reaction was quite rapid, with the solution becoming visibly blue/green in the first minute of the reaction. However, the finely dispersed Cu^0 generated via disproportionation caused significant light scattering and large apparent absorbance in the whole spectral region examined (400−1400 nm, Figure S9). When the cuvette with the solution was left for sufficiently long time (>3 h), allowing the produced Cu^0 to settle, the absorbance was very close to that determined from comproportionation experiments. Figure 2 illustrates the reduction of Cu^{II} species by Cu^0, as determined by monitoring absorption at 970 nm in MeCN ($\epsilon_{970}(Cu^{II}Br_2/Me_6TREN)$ = 439.5 M^{-1} cm^{-1} in the presence of 1−2 equiv of free Me_6TREN), DMSO (ϵ_{970} = 471.7 M^{-1} cm^{-1}), and DMF (ϵ_{970} = 458.1 M^{-1} cm^{-1}) at 25 °C. In MeCN, comproportionation to form $CuBr/Me_6TREN$ was virtually complete, in agreement with earlier observations that $CuBr/Me_6TREN$ is stable toward disproportionation in this solvent.[42] In DMF and DMSO, comproportionation was less efficient (i.e., disproportionation more pronounced). In all cases, the comproportionation process is not fast and takes >1 h to consume 50% of $Cu^{II}Br_2/Me_6TREN$, undoubtedly a product of the heterogeneity of the reaction and influenced by the size and surface area of Cu^0. (A 10% excess of Cu^0 was employed to ensure a sufficient concentration of the species was available to fully comproportionate with $Cu^{II}Br_2$.)

The disproportionation equilibrium not only depends on solvent, ligand, and temperature but can be also affected by the concentration of free ligand. Figure S4 shows the concentration of $CuBr_2$ species remaining in a solution of DMSO after reduction by Cu^0 as a function of variable free ligand concentration. As anticipated from eq 6, the addition of excess ligand enhances comproportionation. The concentration of $Cu^{II}X_2/L$ at equilibrium was used to calculate the disproportionation equilibrium constant according to eq 7. The values of log (K^L_{disp}) obtained from the three experiments were very similar, ranging from −1.0 to −1.5. Additionally, the same value of log(K^L_{disp}) could be obtained either starting only with Cu^IBr/Me_6TREN and following disproportionation or starting with Cu^0/Me_6TREN and $Cu^{II}Br_2/Me_6TREN$ and following comproportionation (Figure 3). The disproportionation equilibrium constant values obtained from all experiments are summarized in Table 1. Caution should be exerted when interpreting the results of model studies intended to quantify disproportionation of Cu^I when it is observed that $[Cu^{II}Br_2]$ at equilibrium has exceeded half the initial value of $[Cu^I]$. This is, needless to say, impossible if disproportionation of Cu^I is the only means by which Cu^{II} is introduced to the system; such an observation (see Supporting Figures 1, 3, 7, 8, 10, 11, 13, 17, 20, and 23 in ref 42) indicates either oxidation of Cu^I by adventitious air or incorrect absorption measurements due to light scattering by Cu^0 particles.

II. Polymerization of Methyl Acrylate (MA). As discussed, control attained in polymerizations of MA conducted in DMSO in the presence of Cu^0/Me_6TREN was ascribed in ref 42 to a mechanism involving exclusive activation of R−X by Cu^0, subsequent generation of Cu^IX/Me_6TREN, and instantaneous disproportionation of the Cu^I species to (re)generate Cu^0 and a Cu^{II} deactivating species. While we have just demonstrated that slow comproportionation of the Cu^IX/Me_6TREN species actually dominates in DMSO, a certain amount of Cu^I will disproportionate under polymerization conditions. We now compare polymerization results for MA in both DMSO and MeCN; in

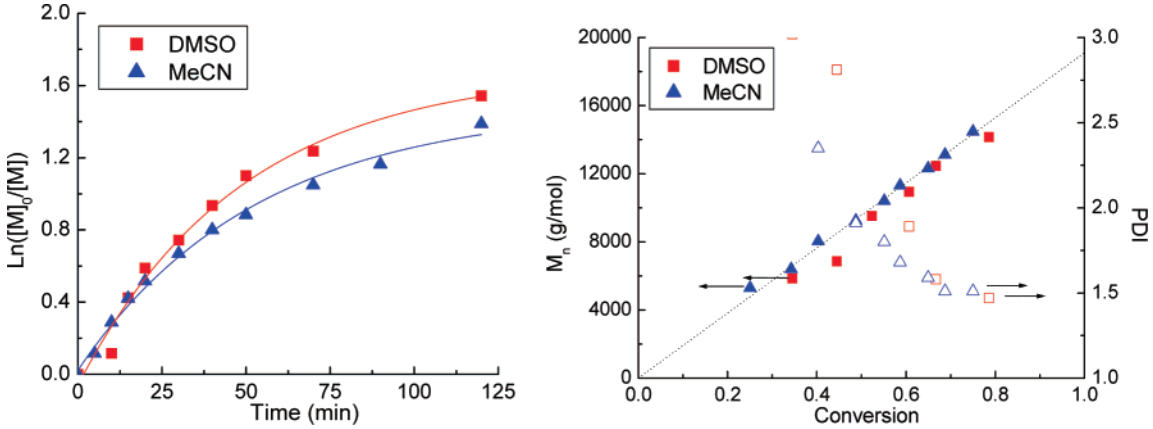

Figure 4. (left) Kinetic plot and (right) plot of M_n and M_w/M_n vs conversion for MA polymerization catalyzed by Cu^0. [MA]/[MBP]/[Cu^0]/[Me_6-TREN] = 222/1/0.1/0.1; 25 °C; MA/DMSO or MeCN = 2/1 v/v.

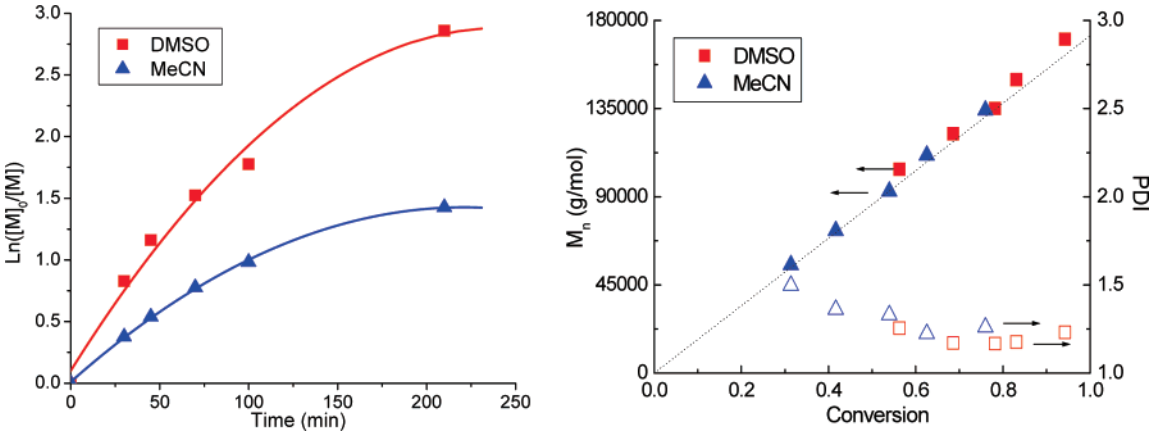

Figure 5. (left) Kinetic plot and (right) plot of M_n and M_w/M_n vs conversion for MA polymerization catalyzed by Cu^0. [MA]/[MBP]/[Cu^0]/[Me_6-TREN] = 2000/1/1/1; 25 °C; MA/DMSO or MeCN = 1/1 v/v.

the latter solvent, disproportionation can essentially be neglected. Additionally, systems based on Cu^0 were compared with those based on Cu^I, from which convincing evidence to support the true polymerization mechanism in the presence of Cu^0 could be deduced.

It must be noted that Cu^IBr/Me_6TREN is among the most active catalysts to have ever been employed in ATRP.[61] As previously reported, bulk polymerization of MA with an equimolar amount of catalyst relative to initiator is extremely fast (for a targeted M_n = 20 000 g/mol) and noticeably exothermic. Without appropriate means to cool the system, the reaction mixture starts boiling within a few minutes.[62] However, when the amount of catalyst is reduced to ~10 mol % vs initiator, better control over polymerization can be achieved. Polymerization of more active ATRP monomers such as methacrylates and styrene with $CuBr/Me_6TREN$ catalyst proves even more challenging.[32]

A. Cu^0-Mediated Polymerization. Figure 4 illustrates the evolution of molecular weights and polydispersities with conversion for the polymerization of MA, initiated by methyl 2-bromopropionate (MBP), targeting low molar mass polymers in the presence of 10% Cu^0 and Me_6TREN relative to MBP, in both MeCN and DMSO. The two polymerizations are well controlled in terms of molecular weights agreeing with theoretical values, although polydispersity is quite high for most of the reaction ($M_w/M_n \geq 1.5$). Given the proposition that two entirely different mechanisms operate under these conditions, with one being "ultrafast", the two polymerizations display an astonishingly similar level of control and overall rate. In both solvents, nonlinear first-order kinetics are observed. Similar curvature in kinetic plots has been observed in ARGET ATRP systems when an insufficient amount of reducing agent (i.e., Cu^0) was available to regenerate the Cu^I activator consumed by termination reactions.

When the concentration of MBP is lowered approximately 10-fold such that a higher molecular weight is targeted and an equimolar amount of Cu^0 and MBP are employed, control over molecular weight is retained, and polydispersity improves significantly (Figure 5). The polymerization rate still begins to slow at higher conversion, which again is consistent with ARGET ATRP for a system with an insufficient amount (or heterogeneous solution) of reducing agent. The same phenomenon is expected for SET-LRP, where Cu^{II} should be accumulated and Cu^0 (activator) consumed.

B. Cu^I-Mediated Polymerization. Polymerization of MA catalyzed by Cu^IBr/Me_6TREN was also compared in both DMSO and MeCN at 25 °C ([MA]/[MBP]/[Cu^IBr]/[Me_6TREN] = 2000/1/1/1 and 222/1/1/1). High conversion could not be reached in any case (Figures 6 and S10). This can partially be attributed to significant termination reactions resulting from a high radical concentration generated by the exceptionally active homogeneous Cu^I catalyst (consistent with previous literature results[62]).

However, detailed analysis of the GPC traces from these reactions in both solvents showed an unusual tailing toward low molar mass and essentially no shoulder at higher molecular weight that would be indicative of radical coupling (Figures 7 and S11). A plausible explanation for the observations is that Cu^IBr/Me_6TREN, a relatively powerful reducing species, can not only activate alkyl halides to generate radicals but can also

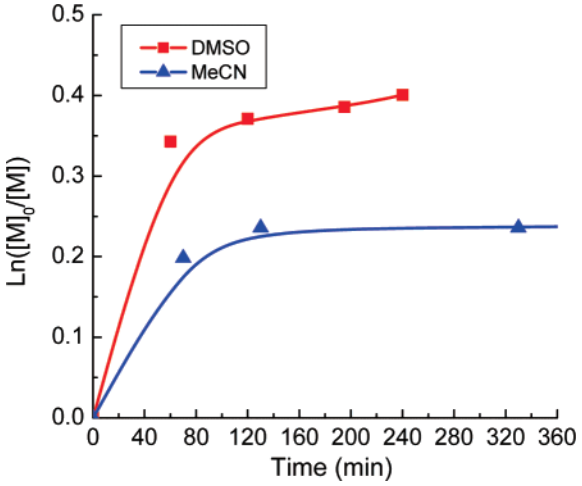

Figure 6. Kinetic plot for MA polymerization with Cu^IBr/Me_6TREN: [MA]/[MBP]/[Cu^IBr]/[Me_6TREN] = 2000/1/1/1 ; 25 °C; MA/DMSO or MeCN = 1/1 v/v.

reduce growing radicals to carbanions that would then react rapidly with adventitious moisture or other protic impurities. This side reaction would occur via outer-sphere electron transfer (OSET) and should depend on the amount of Cu^I species and its relative reducing power.[53] Similar results have previously been observed in acrylate polymerization[61] as well as in the polymerization of other electrophilic monomers such as acrylonitrile[63] when catalyzed by strongly reducing species. The OSET side reaction between Cu^I and radicals can be minimized when a very small amount of catalyst is employed in ARGET ATRP, allowing the production of higher molecular weight polymers of acrylonitrile with less apparent tailing.[64]

Figure S12 illustrates that, by lowering the relative amount of catalyst to initiator to 10% and/or targeting a lower degree of polymerization, good control can be achieved in both DMSO and MeCN, in agreement with earlier reports.[62]

C. Slow Dosing of Cu^I to Polymerization. One approach to suppressing OSET as a side reaction in the presence of strongly reducing Cu^I species is to slowly feed the catalyst to the reaction mixture at a similar rate it is consumed by the persistent radical effect, effectively keeping [Cu^I] low at any given time. A low [Cu^I] would also keep radical concentrations relatively low, thereby reducing the probability of radical termination. Moreover, a major role of Cu^0 in these solvents (as will be discussed in more detail) is as a relatively mild reducing agent working to reduce accumulated Cu^{II} back into Cu^I. Thus, a slow feeding of Cu^IBr/Me_6TREN to a polymerization essentially mimics a system in which Cu^0 slowly reduces $Cu^{II}Br_2/Me_6TREN$.

The experiment was begun with a small amount of $CuBr_2$/Me_6TREN initially present, which ultimately allows better control over the polymerization. Excellent control was observed, as indicated by a linear increase of molecular weight with conversion, low polydispersity (Figure 8), and a smooth evolution of the entire distribution of polymer chains with conversion without any observable tailing (Figure 9). These results essentially mirror those of the Cu^0 experiments.

Additionally, ultrahigh molecular weight PMA (M_n > 2 000 000 g/mol) was synthesized in DMSO with a slow dosing of Cu^I to the system (Figure 10). In MeCN, molecular weights higher than 600 000 g/mol were difficult to obtain due to the relatively high transfer constant between MeCN and a methyl acrylate radical.[65] Together with the model studies demonstrating the propensity of Cu^0 to comproportionate, these results indicate the principal role of Cu^0 is to slowly introduce Cu^I activator back into solution (as in ARGET ATRP).

D. Retention of End-Group Functionality in Cu^0-Mediated Polymerization. It was previously claimed that termination reactions, which would result in a loss of end-group functionality, were below the threshold of what could be detected in Cu^0-mediated polymerization.[42] We attempted to verify this with macroinitiators synthesized using Cu^0 ([MA]/[MBP]/[Cu^0]/[Me_6-TREN] = 222/1/0.1/0.1; 25 °C, in 50 vol % DMSO). Nanosized Cu^0 powder (100 nm) was used, and the reaction was quenched after 5 min, having reached a conversion of 86% with M_n = 16 500 g/mol and M_w/M_n = 1.24.

Despite the relatively narrow molecular weight distribution of the macroinitiator, a significant amount of the chains (Figure 11) could not be extended ([MA]/[macroinitiator]/[Cu^0]/[Me_6-TREN] = 222/1/1/1; 25 °C; MA/DMSO = 1/3 v/v). Initiation efficiency of the chain extension was calculated as only 51% by multipeak analysis and integration of the GPC traces after conversion of the weight distribution to number distribution. (For slower reactions proceeding with a lower radical concentration, chain end functionality is better preserved.)

E. Effect of Cu^0 Size/Age. The size of the Cu^0 particles is known to affect the rate of comproportionation[66] and should also, in principle, affect the rate of and control over polymerization. Metal sheets, turnings, wire, and large particle size powders are expected to catalyze slower polymerizations than very small Cu^0 particles. Table 2 summarizes some results of MA polymerization using various types of Cu^0. Not only the size and surface area of Cu^0 but also its "age" affect the polymerization rate (most likely related to a passivating oxide layer or the amount of pristine Cu^0). While polymerization catalyzed from Cu^0 wire has a broad molecular weight distribution, better control could be obtained with wire in the presence of a small amount of $Cu^{II}Br_2$ complex. Additionally, the difficulty of working with extremely low concentrations of Cu^0 by using stock suspensions when synthesizing high molecular weight polymers is discussed in the Supporting Information and illustrated in Figure S13.

III. Model Studies on Activation Process. In order to better understand all reactions involved and also to estimate the relative contribution of R−X activation by Cu^0 and Cu^I, several model reactions were performed to gain a more comprehensive picture of the Cu^0 system.

A. Activation Rate Constants in the Presence of CuBr/Me_6TREN with and without Cu^0. Activation rate constants for numerous alkyl halides with various copper complexes in ATRP have previously been measured by trapping radicals generated during the activation step with a nitroxide radical in order to avoid the back (deactivation) reaction (Scheme 4).[67]

Cu^I/Me_6TREN is among the most reactive catalysts known in ATRP. Activation is also strongly dependent on the structure of the initiator. At room temperature, k_{act} for benzyl chloride ($PhCH_2Cl$) with Cu^ICl/Me_6TREN is 0.2 M^{-1} s^{-1}, for MBP with Cu^IBr/Me_6TREN k_{act} = 50 M^{-1} s^{-1}, and for ethyl 2-bromophenylacetate with Cu^IBr/Me_6TREN $k_{act} = 6.5 \times 10^5$ M^{-1} s^{-1} (the latter two values were extrapolated by comparison with different ligands).[68] Because the reaction of Cu^I/Me_6TREN with MBP is too fast to measure precisely, the following kinetic studies are conducted with benzyl chloride. Figure 12 presents the kinetics of four reactions of benzyl chloride in MeCN with (a) Cu^0 and Me_6TREN, (b) Cu^ICl/Me_6TREN in the absence of Cu^0, (c) 1 equiv each of Cu^0, Cu^ICl, and Me_6TREN, and (d) 1 equiv of Cu^0 and Cu^ICl with 2 equiv of Me_6TREN. Because activation of an alkyl halide by Cu^0 was not observed to occur without ligand, a sufficient amount of Me_6TREN was employed

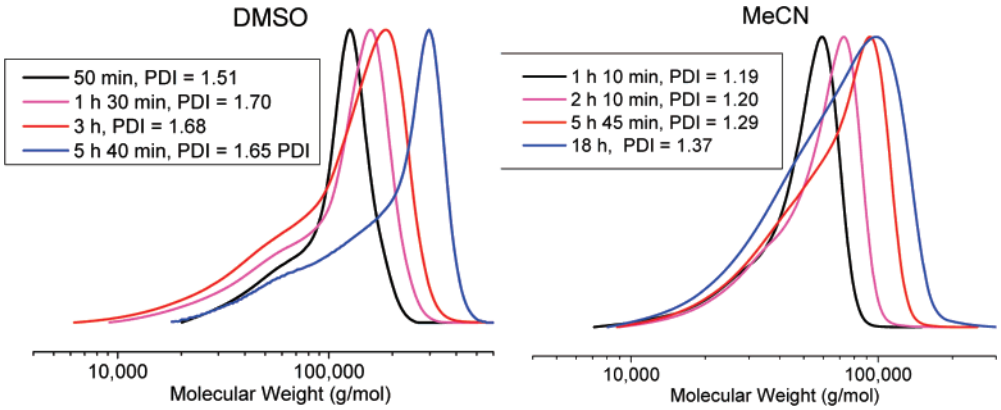

Figure 7. GPC traces illustrating molecular weight evolution during MA polymerization with $Cu^{I}Br/Me_6TREN$: [MA]/[MBP]/[$Cu^{I}Br$]/[Me_6-TREN] = 2000/1/1/1; 25 °C; MA/DMSO or MeCN = 1/1 v/v.

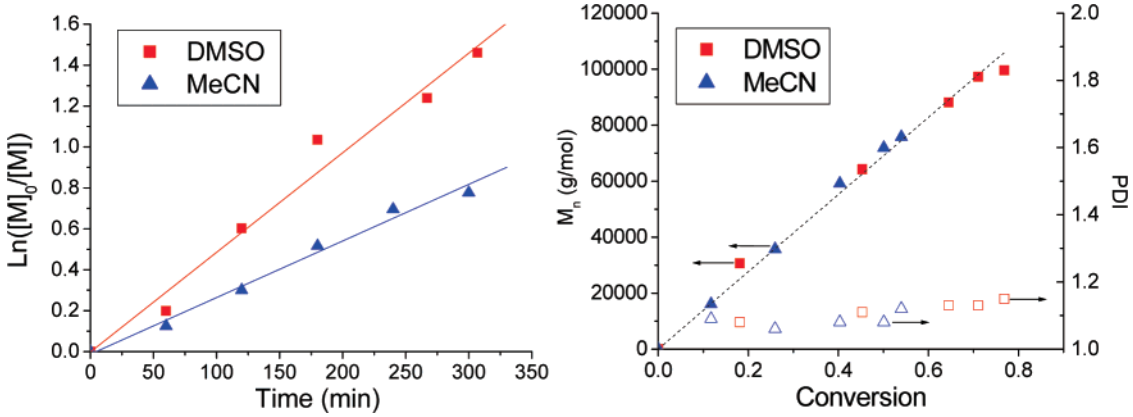

Figure 8. (left) Kinetic plot and (right) plot of M_n and M_w/M_n vs conversion for MA polymerization with a slow feeding of $Cu^{I}Br/Me_6TREN$. Relative concentration of all injected species: [MA]/[MBP]/[$Cu^{I}Br$]/[$Cu^{II}Br_2$]/[Me_6TREN] = 2000/1.25/1/0.05/1.05; 25 °C; MA/DMSO or MeCN = 1/1 v/v. A 2.1 mL solution containing 0.025 mmol $Cu^{I}Br/Me_6TREN$ in DMSO or MeCN was added over 5 h to a system with 4.5 mL of MA, 2.4 mL of solvent, 0.5 mL of anisole (internal standard), and the $Cu^{II}Br_2/Me_6TREN$ and MBP.

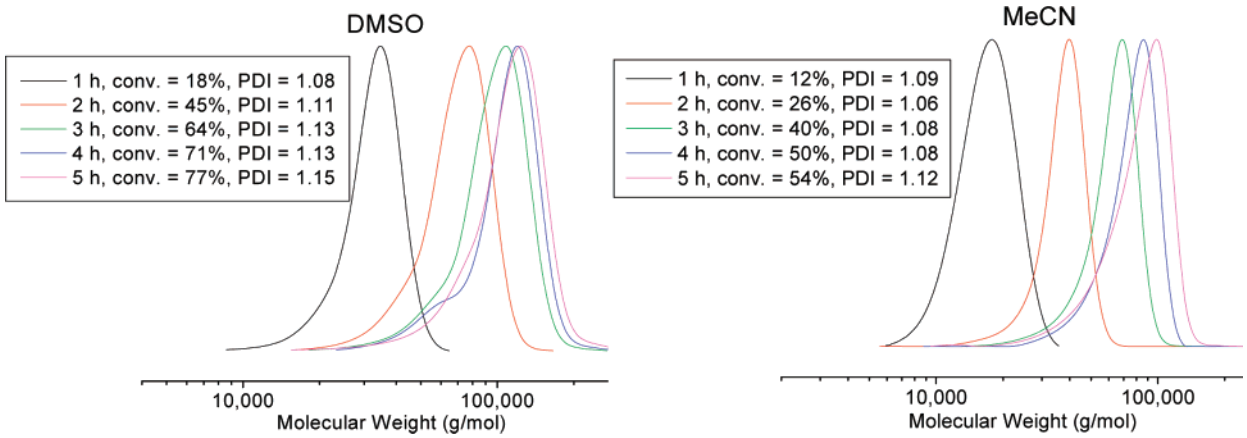

Figure 9. GPC traces illustrating molecular weight evolution for MA polymerization with a slow feeding of $Cu^{I}Br/Me_6TREN$. [MA]/[MBP/[$Cu^{I}Br$]/[$CuBr_2$]/[Me_6TREN] = 2000/1.25/1/0.05/1.05; 25 °C; MA/DMSO or MeCN = 1/1 v/v.

whenever Cu^0 was used. In all experiments, the nitroxide radical TEMPO was used in excess as the trapping species.

Straight semilogarithmic plots were observed in all experiments initially employing Cu^I. The initial rates were essentially the same with and without the presence of Cu^0. Also, the initial rate with Cu^0 alone was very slow, although it became progressively faster until it matched the rates of the other experiments as Cu^I activator was slowly generated and later regenerated through comproportionation. The data therefore clearly demonstrate that the activation process, regardless of whether polymerization was initially catalyzed by Cu^0 or Cu^I, ultimately occurs predominantly with Cu^I and not with Cu^0 in MeCN.

B. Reaction of $PhCH_2Cl$ with Cu^0/Me_6TREN in the Absence of a Nitroxide Radical Trap. While trapping radicals with TEMPO in the previous experiment allowed a straightforward evaluation of activation kinetics, further insight into the complexity of the reaction of $PhCH_2Cl$ with Cu^0 could be attained in the absence of a radical trap. The consumption of alkyl halide was monitored by gas chromatography while [Cu^{II}] was simultaneously determined with spectrophotometric measurements. From the material balance of all reagents involved,

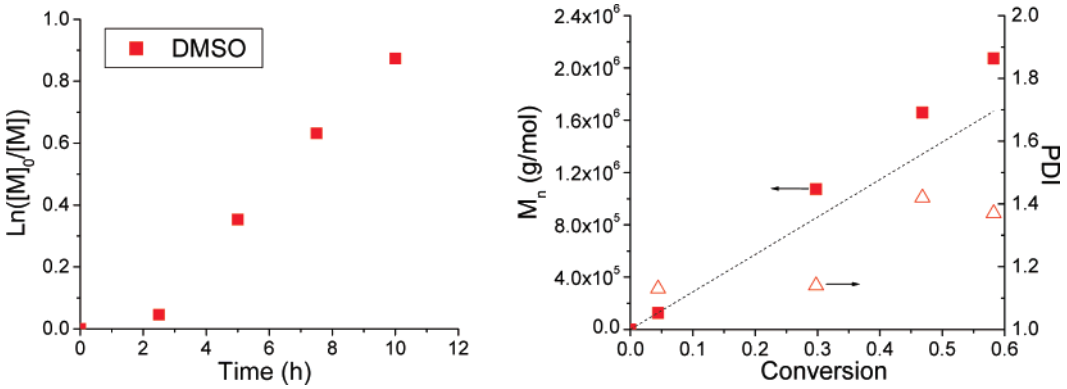

Figure 10. (left) Kinetic plot and (right) plot of M_n and M_w/M_n vs conversion for MA polymerization with a slow feeding of Cu^IBr/Me_6TREN. Relative concentration of all injected species: [MA]/[MBP]/[Cu^IBr]/[$Cu^{II}Br_2$]/[Me_6TREN] = 33300/1/1.5/0.05/1.55; 25 °C; MA/DMSO ~1/4 v/v. A 1.5 mL solution containing 0.005 mmol of Cu^IBr/Me_6TREN in DMSO was added over 10 h to a system with 15 mL of MA, 60 mL of DMSO, 7.5 mL of anisole (internal standard), and the $Cu^{II}Br_2/Me_6TREN$ and MBP.

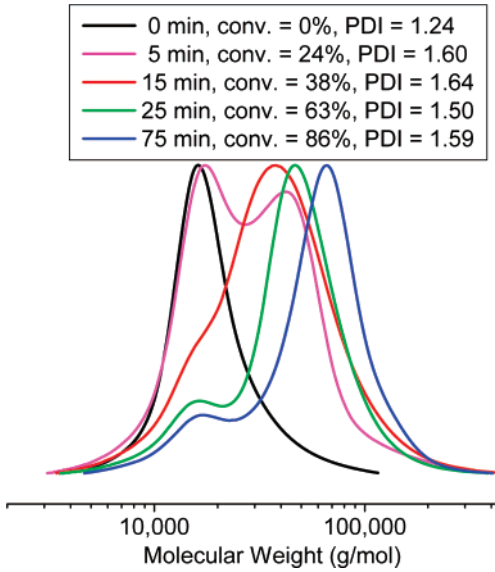

Figure 11. GPC traces illustrating molecular weight evolution for MA chain extension from a macroinitiator prepared with nanosized Cu^0. [MA]/[macroinitiator]/[Cu^0]/[Me_6TREN] = 222/1/1/1; 25 °C; MA/DMSO = 1/3 v/v.

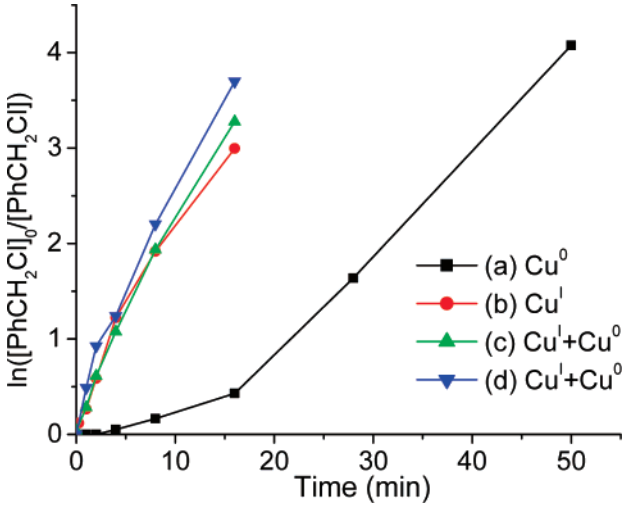

Figure 12. Kinetics of the activation process of benzyl chloride by Cu^X/Me_6TREN in the presence of TEMPO at room temperature in MeCN; [TEMPO] = 20 mM, [$PhCH_2Cl$] = 2 mM, [trichlorobenzene] = 2 mM; (a) and (b) [Cu^X] = [Me_6TREN] = 20 mM; (c) [Cu^0] = [Cu^I] = [Me_6TREN] = 20 mM; (d) [Cu^0] = [Cu^I] = 20 mM, [Me_6TREN] = 40 mM.

it was possible to calculate the concentration of the Cu^I species ([Cu^I] = Δ[RX] − 2[Cu^{II}]), and in a similar manner the residual Cu^0 ([Cu^0] = [RX] + [Cu^{II}] + ([Cu^0]$_0$ − [RX]$_0$), where the latter term is employed since a slight excess of Cu^0 to RX is used; Figure 13). These model reactions are only qualitatively discussed here. In a following paper, a kinetic modeling approach will be employed to fit all relevant rate constants, including the rate of comproportionation, and to quantitatively compare activation rate constants for Cu^0 and Cu^I species.

It is clearly observed in Figure 13 that the concentration of Cu^{II} passes through a maximum and then decreases to a certain equilibrium value. Additionally, Cu^I is constantly accumulated, even after the alkyl halide is consumed. This is consistent with the slow comproportionation process. Similar results were obtained when MBP was employed as the initiator (Figure S14).

IV. Outer-Sphere Electron Transfer (OSET) vs Inner-Sphere Electron Transfer (ISET). While it is generally accepted that activation in ATRP, or oxidation of the Cu species, is accompanied by atom transfer in a concerted ISET process under typical conditions with Cu-based catalysts (Scheme 5), further support for this mechanism is provided with electrochemical arguments below. If the catalyst was sufficiently reducing and alkyl halides had sufficient electron affinity, an

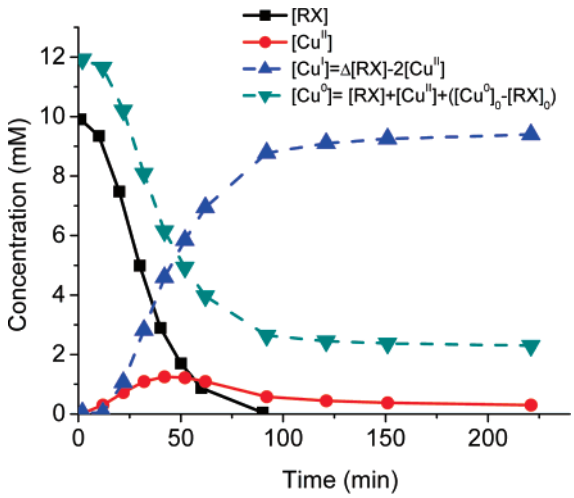

Figure 13. Time-dependent concentration of Cu species and $PhCH_2Cl$ in MeCN as determined by gas chromatography and spectrophotometric measurements. [Cu^0]/[Me_6TREN]/[$PhCH_2Cl$]/[trichlorobenzene] = 12/10/10/10 mM.

outer-sphere electron transfer (OSET) might also be possible. OSET can either occur stepwise or in a concerted fashion.[69,70] For aromatic halides,[71] it can proceed in two steps: (1) the

Table 2. Effect of Size/Age of Cu^0 on ATRP of MA in DMSO at 25 °C[a]

	MA/I/Cu^0/L	time (min)	conversion (%)	M_n (g/mol)	PDI	$M_{n,th}$ (g/mol)
100 nm	222/1/1/1	3.5	79	17 400	1.12	15 300
75 μm	222/1/1/1	8	82	19 800	1.24	15 800
425 μm	222/1/1/1	30	87	20 300	1.24	16 800
40 μm (old)	222/1/1/0.5	75	86	23 400	1.23	16 600
75 μm	222/1/1/0.5	9	86	20 600	1.26	16 600
wire (L = 2 cm, D = 1 mm)	222/1/15/1	90	70	13 600	1.44	13 500
wire (L = 2 cm, D = 1 mm)	222/1/15/1/0.1 $Cu^{II}Br_2$	120	78	15 100	1.06	15 100

[a] I = initiator MBrP; L = ligand Me_6TREN; in 25 °C; MA/DMSO = 1/1 v/v.

aromatic halide accepts an electron to form a radical anion with an oxidized metal cation, and (2) heterolytic dissociation of the radical anion occurs to generate an organic radical R• and a halide anion X^- that migrates to the oxidized metal center (Scheme 5). However, for most alkyl halides,[72,73] OSET occurs in one concerted step directly to form R• and X^- (also known as dissociative electron transfer, or DET) without the generation of an intermediate radical anion species. Moreover, since the redox potentials of many radicals with electron-withdrawing groups (carbomethoxy or cyano) are much less negative that those of the corresponding alkyl halides, the radicals can be irreversibly reduced to carbanions.[73]

The authors of ref 42 measured apparent rate constants of propagation for acrylate polymerizations using chloroform, bromoform, and iodoform initiators with Cu^0 and cited the relative independence of the rate of propagation on the nature of the halogen as evidence for an OSET mechanism. However, according to literature,[73] iodoacetonitrile is reduced ~1000 times faster than bromoacetonitrile and the latter ~1000 times faster than chloroacetonitrile, using the same homogeneous reducing agents. The peak potentials under heterogeneous conditions are −1.24, −1.58, and −2.0 V, respectively, vs SCE, confirming the strong dependence of the reduction potential on the nature of the halide.[72] (0.059 V corresponds to 1 order of magnitude in the equilibrium constant of electron transfer at room temperature.) By contrast, differences in reactivity of alkyl halides are much smaller in atom transfer processes. Alkyl bromides are on average only ~20 times more active than alkyl chlorides, and methyl 2-iodopropionate is only 1.5 times more reactive than methyl 2-bromopropionate.[68] Thus, similar reactivities of haloforms reported in ref 42 indicate ISET rather than OSET occurs under the conditions reported.

Scheme 4. Trapping of Alkyl Radicals with Nitroxide Radicals

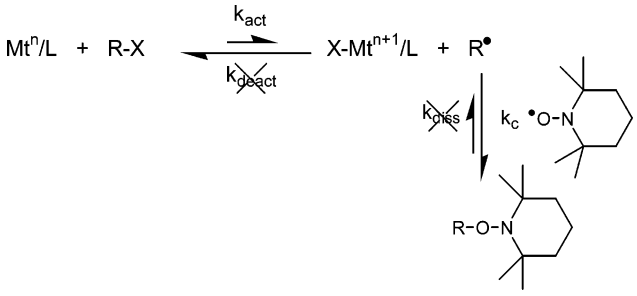

Scheme 5. ISET vs OSET Processes

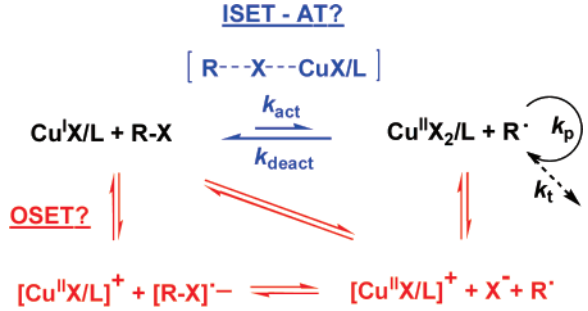

The results of a recent DFT study (where only enthalpy was calculated in the gas phase)[74] were interpreted to suggest that electron transfer to alkyl halides proceeds stepwise with the formation of radical anions being more stable by 7 ± 2 kcal/mol than the radical and halide pair that would form by dissociative electron transfer. However, entropy was not taken into account in these calculations. (Dissociation of a radical anion generates three degrees of translational freedom to form a radical and anion.) The typical entropy gain for the dissociation step should be ~30 cal/mol K, corresponding to about 10 kcal/mol at room temperature. Given the thermodynamic instability of the radical anion species, a one-step DET rather than a two-step process involving a radical anion intermediate should be favored in OSET. Moreover, all calculations[74] were performed in the gas phase. In solution, solvation of halide anions should further stabilize these species.[75,76] It was also reported that the products of homolytic cleavage of alkyl halides (R• and X•) are energetically less favored than the products of the heterolytic cleavage (R• and X^-). However, the difference between the energies of both states reflects only the electron affinity of halogens and has no correlation with the energetics of the ISET and OSET processes illustrated in Scheme 5.

Below, information on the redox properties of all species involved in the polymerization, including Cu in all its oxidation states as well as R−X and R•, is used in an effort to differentiate OSET and ISET processes. We[77] and others[78] have measured the redox properties of various Cu^{II}/Cu^{I} complexes in MeCN, and they are generally in the range of +0.1 to −0.3 V vs SCE (cf. Table 3). Unfortunately, information on the redox potentials of R−X and R• is quite limited.[79] Nevertheless, Table 3 does include some (irreversible) reduction peak potentials for several alkyl halides as well as organic radicals. While precise thermodynamic information cannot be attained from irreversible data, some relevant trends still merit discussion.

The location of the reduction peak of R−X depends strongly on the nature of the halide, occurring between −2.0 and −1.3

Table 3. Redox Potentials of Cu Catalysts, Alkyl Halides, and Organic Radicals[a]

compound	$E_{1/2}$, V (MeCN)	ref
Cu^IBr/Me_6TREN	−0.300	77
Cu^IBr/TPMA	−0.245	77
Cu^IBr/PMDETA	−0.075	77
$Cu^IBr/(bpy)_2$	0.035	77
$NCCH_2$•	−0.69 (E_p, DMF)	73
$PhCH_2$•	−1.45 (E_p)	80
$PhCH_2Br$	−1.80 (E_p)	81
ICH_2CN	−1.24 (E_p, DMF)	72
$BrCH_2CN$	−1.60 (E_p, DMF)	72
$ClCH_2CN$	−2.00 (E_p, DMF)	72
EtClOAc	−2.05 (E_p, DMF)	82

[a] All potentials given vs SCE; E_p = irreversible reduction peak; Me_6TREN = tris[2-(dimethylamino)ethyl]amine, TPMA = tris[(2-pyridyl)-methyl]amine, PMDETA = *N*,*N*′,*N*″,*N*‴,*N*‴-pentamethyldiethylenetriamine, bpy = 2,2′-bipyridine, EtClOAc = ethyl chloroacetate.

Scheme 6. OSET in the Presence of Protic Impurities

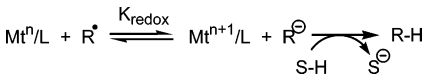

V for haloacetonitrile (vs SCE in DMF).[72] The $^{\bullet}CH_2CN$ species is much easier to be reduced (−0.69 V) than the analogous alkyl halide.[73] Similarly, the reduction peak of benzyl bromide occurs at −1.80 V, while $PhCH_2^{\bullet}$ is reduced at −1.45 V. This is a general trend for R−X employed in ATRP and their corresponding radicals. It suggests that if activation of R−X by Cu^0 were to proceed via OSET (as has been proposed for the SET-LRP system), polymerization might be accompanied by a loss of chain end functionality from reduction to carbanions (see Scheme 6), which would quickly terminate in the presence of adventitious moisture and would further result in a broad molecular weight distribution from significant "tailing" in the GPC traces.

Indeed, such tailing is observed when the ATRP of electrophilic monomers (such as acrylonitrile and acrylates) are catalyzed by very active/reducing Cu^I catalysts under normal ATRP conditions (cf. also Figure 7).[53] This has been attributed to OSET from the catalyst to $R^{\bullet}$. However, much higher molecular weights with less tailing could be achieved under ARGET ATRP conditions, where catalyst concentrations are smaller and consequently OSET to radical chain ends is much less pronounced.[64] The fact that perfectly monomodal distributions of high molecular weight acrylate polymers have reportedly been achieved when catalyzed by Cu^0 suggests OSET to $R^{\bullet}$ is not significant, and is even less likely with less oxidizing RX.

Conclusions

Overall, the results presented in this work demonstrate that methyl acrylate polymerization mediated by Cu^0 resembles the ARGET ATRP mechanism in the organic solvents investigated. Activation occurs predominantly with Cu^I while Cu^0 contributes to the activation process only to a small degree. Cu^0 also works to slowly reduce (i.e., comproportionate with) Cu^{II}, thereby regulating the ratio of Cu^I activator to Cu^{II} deactivator. Some more detailed conclusions include the following:

(1) Disproportionation is limited in DMSO and DMF, and it is negligible in MeCN. When 2.5 mM $Cu^{II}Br_2/Me_6TREN$ is dissolved in the presence of a 10% excess of Cu^0 and sufficient excess of ligand, 28%, 10%, and <1% of Cu^{II} remains after equilibrium is reached in DMSO, DMF, and MeCN, respectively. Comproportionation dominates but is slow due to the heterogeneity of the system.

(2) Rates and control in polymerizations starting with Cu^I or Cu^0 in either DMSO or MeCN are similar. Cu^0/Me_6TREN ultimately catalyzes a more efficient polymerization than Cu^I/Me_6TREN, since the heterogeneous complex reacts more slowly with R−X and does not generate too many radicals. An important role of Cu^0 is to regenerate Cu^I and balance the ratio of $[Cu^I]/[Cu^{II}]$.

(3) A slow dosing of Cu^I activator to the polymerization provides very similar control and mimics a system starting with Cu^0, which slowly reduces Cu^{II} thereby reintroducing Cu^I to the polymerization.

(4) The nature of Cu^0, in terms of the size and surface quality, can affect the kinetics and control.

(5) Model reactions indicate that alkyl halides react much faster with $CuBr/Me_6TREN$ than with Cu^0 and Me_6TREN in MeCN, even though Cu^0/Me_6TREN is more reducing in this solvent. This was attributed to the relatively small surface area and the heterogeneous nature of Cu^0. We also observed the continuous generation of Cu^I throughout a reaction of R−X with Cu^0/Me_6TREN via the slow reduction of accumulated Cu^{II}.

(6) The side reaction of OSET between catalysts and propagating radicals can be lowered under ARGET ATRP conditions, where the catalyst concentration is minimized, thereby allowing the production of higher molecular weight polymers than can be attained under normal ATRP conditions.

(7) The predominant involvement of Cu^0 in the activation process violates the principle of microscopic reversibility, which would otherwise require fast deactivation of propagating radicals by Cu^IBr/Me_6TREN to reversibly form Cu^0.

(8) All of the experimental observations can be fully explained by the existing ATRP mechanism, wherein Cu^0 acts as a reducing agent and can also contribute to the activation process. The proposed involvement of unquantifiable "nascent" atomic Cu^0 as the most likely activator is therefore unwarranted (cf. Occam's razor).

Acknowledgment. The authors thank the National Science Foundation (DMR-05-49353 and CHE-07-15494) and the members of the CRP Consortium at Carnegie Mellon University for their financial support as well as the entire Matyjaszewski group for helpful discussions and experimental assistance. We thank one of the reviewers for helpful comments concerning the PMR.

Supporting Information Available: Electronic spectra for all comproportionation and disproportionation experiments as well as kinetic plots, M_n and M_w/M_n vs conversion data, and GPC traces for select polymerizations. This material is available free of charge via the Internet at http://pubs.acs.org.

References and Notes

(1) Matyjaszewski, K.; Davis, T. P. *Handbook of Radical Polymerization*; Wiley-Interscience: Hoboken, NJ, 2002.
(2) Matyjaszewski, K., Ed. *Controlled/Living Radical Polymerization: From Synthesis to Materials*; ACS Symp. Ser. 944; American Chemical Society: Washington, DC, 2006.
(3) Matyjaszewski, K., Gnanou, Y., Leibler, L., Eds. *Macromolecular Engineering: From Precise Macromolecular Synthesis to Macroscopic Materials, Properties and Applications*; Wiley-VCH: Weinheim, 2007.
(4) Braunecker, W. A.; Matyjaszewski, K. *Prog. Polym. Sci.* **2007**, *32*, 93−146.
(5) Wang, J.-S.; Matyjaszewski, K. *J. Am. Chem. Soc.* **1995**, *117*, 5614−5615.
(6) Patten, T. E.; Matyjaszewski, K. *Adv. Mater.* **1998**, *10*, 901−915.
(7) Matyjaszewski, K. *Chem.—Eur. J.* **1999**, *5*, 3095−3102.
(8) Coessens, V.; Pintauer, T.; Matyjaszewski, K. *Prog. Polym. Sci.* **2001**, *26*, 337−377.
(9) Matyjaszewski, K.; Xia, J. *Chem. Rev.* **2001**, *101*, 2921−2990.
(10) Kamigaito, M.; Ando, T.; Sawamoto, M. *Chem. Rev.* **2001**, *101*, 3689−3745.
(11) Pyun, J.; Matyjaszewski, K. *Chem. Mater.* **2001**, *13*, 3436−3448.
(12) Davis, K. A.; Matyjaszewski, K. *Adv. Polym. Sci.* **2002**, *159*, 1−166.
(13) Matyjaszewski, K. *Polym. Int.* **2003**, *52*, 1559−1565.
(14) Wang, J.-S.; Matyjaszewski, K. *Macromolecules* **1995**, *28*, 7901−7910.
(15) Matyjaszewski, K.; Beers, K. L.; Kern, A.; Gaynor, S. G. *J. Polym. Sci., Part A: Polym. Chem.* **1998**, *36*, 823−830.
(16) Zhang, X.; Xia, J.; Matyjaszewski, K. *Macromolecules* **1998**, *31*, 5167−5169.
(17) Teodorescu, M.; Matyjaszewski, K. *Macromolecules* **1999**, *32*, 4826−4831.
(18) Wakioka, M.; Baek, K.-Y.; Ando, T.; Kamigaito, M.; Sawamoto, M. *Macromolecules* **2002**, *35*, 330−333.
(19) Paik, H. J.; Gaynor, S. G.; Matyjaszewski, K. *Macromol. Rapid Commun.* **1998**, *19*, 47−52.
(20) Matyjaszewski, K.; Jo, S. M.; Paik, H.-j.; Gaynor, S. G. *Macromolecules* **1997**, *30*, 6398−6400.
(21) Jakubowski, W.; Matyjaszewski, K. *Angew. Chem., Int. Ed.* **2006**, *45*, 4482−4486.
(22) Matyjaszewski, K.; Jakubowski, W.; Min, K.; Tang, W.; Huang, J.; Braunecker, W. A.; Tsarevsky, N. V. *Proc. Natl. Acad. Sci. U.S.A.* **2006**, *103*, 15309−15314.

(23) Tsarevsky, N. V.; Matyjaszewski, K. *Chem. Rev.* **2007**, *107*, 2270−2299.
(24) Matyjaszewski, K.; Spanswick, J. *Mater. Today* **2005**, *8*, 26−33.
(25) Matyjaszewski, K.; Patten, T. E.; Xia, J. *J. Am. Chem. Soc.* **1997**, *119*, 674−680.
(26) Ohno, K.; Goto, A.; Fukuda, T.; Xia, J.; Matyjaszewski, K. *Macromolecules* **1998**, *31*, 2699−2701.
(27) Goto, A.; Fukuda, T. *Prog. Polym. Sci.* **2004**, *29*, 329−385.
(28) Fischer, H. *Chem. Rev.* **2001**, *101*, 3581−3610.
(29) Tang, W.; Tsarevsky, N. V.; Matyjaszewski, K. *J. Am. Chem. Soc.* **2006**, *128*, 1598−1604.
(30) Matyjaszewski, K.; Coca, S.; Gaynor, S. G.; Wei, M.; Woodworth, B. E. *Macromolecules* **1997**, *30*, 7348−7350.
(31) Matyjaszewski, K.; Beers, K. L.; Woodworth, B.; Metzner, Z. *J. Chem. Educ.* **2001**, *78*, 547−550.
(32) Queffelec, J.; Gaynor, S. G.; Matyjaszewski, K. *Macromolecules* **2000**, *33*, 8629−8639.
(33) Matyjaszewski, K.; Coca, S.; Gaynor, S. G.; Wei, M.; Woodworth, B. E. *Macromolecules* **1998**, *31*, 5967−5969.
(34) Woodworth, B. E.; Metzner, Z.; Matyjaszewski, K. *Macromolecules* **1998**, *31*, 7999−8004.
(35) Jakubowski, W.; Min, K.; Matyjaszewski, K. *Macromolecules* **2006**, *39*, 39−45.
(36) Pietrasik, J.; Dong, H.; Matyjaszewski, K. *Macromolecules* **2006**, *39*, 6384−6390.
(37) Tang, H.; Radosz, M.; Shen, Y. *Macromol. Rapid Commun.* **2006**, *27*, 1127−1131.
(38) Matyjaszewski, K.; Dong, H.; Jakubowski, W.; Pietrasik, J.; Kusumo, A. *Langmuir* **2007**, *23*, 4528−4531.
(39) Min, K.; Gao, H.; Matyjaszewski, K. *Macromolecules* **2007**, *40*, 1789−1791.
(40) Percec, V.; Popov, A. V.; Ramirez-Castillo, E.; Monteiro, M.; Barboiu, B.; Weichold, O.; Asandei, A. D.; Mitchell, C. M. *J. Am. Chem. Soc.* **2002**, *124*, 4940−4941.
(41) Percec, V.; Popov, A. V.; Ramirez-Castillo, E.; Weichold, O. *J. Polym. Sci., Part A: Polym. Chem.* **2003**, *41*, 3283−3299.
(42) Percec, V.; Guliashvili, T.; Ladislaw, J. S.; Wistrand, A.; Stjerndahl, A.; Sienkowska, M. J.; Monteiro, M. J.; Sahoo, S. *J. Am. Chem. Soc.* **2006**, *128*, 14156−14165.
(43) Xia, J.; Matyjaszewski, K. *Macromolecules* **1997**, *30*, 7692−7696.
(44) Percec, V.; Barboiu, B.; van der Sluis, M. *Macromolecules* **1998**, *31*, 4053−4056.
(45) Van der Sluis, M.; Barboiu, B.; Pesa, N.; Percec, V. *Macromolecules* **1998**, *31*, 9409−9412.
(46) Tolman, R. C. *Proc. Natl. Acad. Sci. U.S.A.* **1925**, *11*, 436−439.
(47) Chandrasekhar, S. *Res. Chem. Intermed.* **1992**, *17*, 173−209.
(48) Colquhoun, D.; Dowsland, K. A.; Beato, M.; Plested, A. J. R. *Biophys. J.* **2004**, *86*, 3510−3518.
(49) Matyjaszewski, K.; Woodworth, B. E. *Macromolecules* **1998**, *31*, 4718−4723.
(50) Matyjaszewski, K.; Paik, H.-j.; Zhou, P.; Diamanti, S. J. *Macromolecules* **2001**, *34*, 5125−5131.
(51) Gromada, J.; Matyjaszewski, K. *Macromolecules* **2002**, *35*, 6167−6173.
(52) Ciampolini, M.; Nardi, N. *Inorg. Chem.* **1966**, *5*, 41−44.
(53) Tsarevsky, N. V.; Braunecker, W. A.; Matyjaszewski, K. *J. Organomet. Chem.* **2007**, *692*, 3212−3222.
(54) Anderegg, G. *Helv. Chim. Acta* **1963**, *46*, 2397−2410.
(55) Ciavatta, L.; Ferri, D.; Palombari, R. *J. Inorg. Nucl. Chem.* **1980**, *42*, 593−598.
(56) Ahrland, S.; Nilsson, K.; Tagesson, B. *Acta Chem. Scand. A* **1983**, *37*, 193−201.
(57) Lewandowski, A.; Malinska, J. *Electrochim. Acta* **1989**, *34*, 333−335.
(58) Foll, A.; Le, Demezet, M.; Courtot-Coupez, J. *J. Electroanal. Chem.* **1972**, *35*, 41−54.
(59) Ahrland, S.; Blauenstein, P.; Tagesson, B.; Tuhtar, D. *Acta Chem. Scand. A* **1980**, *34*, 265−272.
(60) Malyszko, J.; Scendo, M. *Monatsh. Chem.* **1987**, *118*, 435−443.
(61) Tsarevsky, N. V.; Braunecker, W. A.; Tang, W.; Brooks, S. J.; Matyjaszewski, K.; Weisman, G. R.; Wong, E. H. *J. Mol. Catal. A: Chem.* **2006**, *257*, 132−140.
(62) Xia, J.; Gaynor, S. G.; Matyjaszewski, K. *Macromolecules* **1998**, *31*, 5958−5959.
(63) Matyjaszewski, K.; Jo, S. M.; Paik, H.-j.; Shipp, D. A. *Macromolecules* **1999**, *32*, 6431−6438.
(64) Dong, H.; Tang, W.; Matyjaszewski, K. *Macromolecules* **2007**, *40*, 2974−2977.
(65) Raghuram, P. V. T.; Nandi, U. S. *J. Polym. Sci., Polym. Chem. Ed.* **1970**, *8*, 3079−3088.
(66) Kajiwara, A.; Matyjaszewski, K.; Kamachi, M. *Macromolecules* **1998**, *31*, 5695−5701.
(67) Tang, W.; Matyjaszewski, K. *Macromolecules* **2006**, *39*, 4953−4959.
(68) Tang, W.; Matyjaszewski, K. *Macromolecules* **2007**, *40*, 1858−1863.
(69) Andrieux, C. P.; Le Gorande, A.; Saveant, J. M. *J. Am. Chem. Soc.* **1992**, *114*, 6892−6904.
(70) Saveant, J. M. *Adv. Phys. Org. Chem.* **2000**, *35*, 117−192.
(71) Andrieux, C. P.; Blocman, C.; Dumas-Bouchiat, J. M.; Saveant, J. M. *J. Am. Chem. Soc.* **1979**, *101*, 3431−3441.
(72) Cardinale, A.; Isse, A. A.; Gennaro, A.; Robert, M.; Saveant, J.-M. *J. Am. Chem. Soc.* **2002**, *124*, 13533−13539.
(73) Isse, A. A.; Gennaro, A. *J. Phys. Chem. A* **2004**, *108*, 4180−4186.
(74) Guliashvili, T.; Percec, V. *J. Polym. Sci., Part A: Polym. Chem.* **2007**, *45*, 1607−1618.
(75) Yamdagni, R.; Kebarle, P. *J. Am. Chem. Soc.* **1972**, *94*, 2940−2943.
(76) Magnera, T. F.; Caldwell, G. W.; Sunner, J.; Ikuta, S.; Kebarle, P. *J. Am. Chem. Soc.* **1984**, *106*, 6140−6146.
(77) Qiu, J.; Matyjaszewski, K.; Thouin, L.; Amatore, C. *Macromol. Chem. Phys.* **2000**, *201*, 1625−1631.
(78) Coullerez, G.; Malmstrom, E.; Jonsson, M. *J. Phys. Chem. A* **2006**, *110*, 10355−10360.
(79) Daasbjerg, K.; Pedersen, S. U.; Lund, H. In *General Aspects of the Chemistry of Radicals*; Alfassi, Z. B., Ed.; Wiley: Chichester, 1999; pp 385−427.
(80) Wayner, D. D. M.; McPhee, D. J.; Griller, D. *J. Am. Chem. Soc.* **1988**, *110*, 132−137.
(81) Isse, A. A.; De Giusti, A.; Gennaro, A.; Falciola, L.; Mussini, P. R. *Electrochim. Acta* **2006**, *51*, 4956−4964.
(82) Moad, A. J.; Klein, L. J.; Peters, D. G.; Karty, J. A.; Reilly, J. P. *J. Electroanal. Chem.* **2002**, *531*, 163−169.

MA0717800